batteries

MDPI

Article

# Vanadium Electrolyte for All-Vanadium Redox-Flow Batteries: The Effect of the Counter Ion

**Nataliya Roznyatovskaya [1,2,*], Jens Noack [1,2], Heiko Mild [1], Matthias Fühl [1], Peter Fischer [1,2], Karsten Pinkwart [1,2], Jens Tübke [1,2] and Maria Skyllas-Kazacos [2,3]**

1 Applied Electrochemistry, Fraunhofer Institute for Chemical Technology, Joseph-von-Fraunhofer-Str. 7, 76327 Pfinztal, Germany; jens.noack@ict.fraunhofer.de (J.N.); mild.heiko@gmail.com (H.M.); matthias.fuehl@ict.fraunhofer.de (M.F.); peter.fischer@ict.fraunhofer.de (P.F.); karsten.pinkwart@ict.fraunhofer.de (K.P.); jens.tuebke@ict.fraunhofer.de (J.T.)

2 German-Australian Alliance for Electrochemical Technologies for Storage of Renewable Energy (CENELEST), Mechanical and Manufacturing Engineering, University of New South Wales (UNSW), UNSW Sydney, NSW 2052, Australia; m.kazacos@unsw.edu.au

3 Mechanical and Manufacturing Engineering, University of New South Wales (UNSW), UNSW Sydney, NSW 2052, Australia

* Correspondence: nataliya.roznyatovskaya@ict.fraunhofer.de; Tel.: +49-721-4640659

Received: 17 December 2018; Accepted: 13 January 2019; Published: 18 January 2019


**Abstract:** In this study, 1.6 M vanadium electrolytes in the oxidation forms V(III) and V(V) were prepared from V(IV) in sulfuric (4.7 M total sulphate), V(IV) in hydrochloric (6.1 M total chloride) acids, as well as from 1:1 mol mixture of V(III) and V(IV) (denoted as $V^{3.5+}$) in hydrochloric (7.6 M total chloride) acid. These electrolyte solutions were investigated in terms of performance in vanadium redox flow battery (VRFB). The half-wave potentials of the V(III)/V(II) and V(V)/V(IV) couples, determined by cyclic voltammetry, and the electronic spectra of V(III) and V(IV) electrolyte samples, are discussed to reveal the effect of electrolyte matrix on charge-discharge behavior of a 40 $cm^2$ cell operated with 1.6 M $V^{3.5+}$ electrolytes in sulfuric and hydrochloric acids. Provided that the total vanadium concentration and the conductivity of electrolytes are comparable for both acids, respective energy efficiencies of 77% and 72–75% were attained at a current density of 50 $mA{\cdot}cm^{-2}$. All electrolytes in the oxidation state V(V) were examined for chemical stability at room temperature and +45 °C by titrimetric determination of the molar ratio V(V):V(IV) and total vanadium concentration.

**Keywords:** vanadium redox-flow battery; electrolyte; vanadium redox reactions; electrolyte stability

## 1. Introduction

The electrolyte, as a component of all-vanadium redox flow batteries (VRFBs), contains salts of vanadium dissolved in acids to provide ionic conductivity and enable electrochemical reactions. The charge-discharge process of VRFBs is commonly represented by a combination of the following half-cell reactions:

$$\text{(cathode) } VO_2^+ + e^- + 2H^+ \rightarrow VO^{2+} + 2H_2O \; E^0 = 0.99 \text{ V} \quad (1)$$

$$\text{(anode) } V^{2+} - e^- \rightarrow V^{3+} \; E^0 = -0.26 \text{ V} \quad (2)$$

These reactions depict the charge and mass balance, but the counter ions are usually omitted and not considered, even though the vanadium species are ion-paired with sulfate counter ions at battery-relevant vanadium concentrations, i.e., over the one-molar range in the case of common

sulfuric acid VRFB electrolytes [1–4]. Therefore, the electrochemical kinetics of vanadium reactions, and ultimately the activation losses during battery operation, are likely also dependent on the nature of the counter ion or battery chemistry. The chemistries of VRFB electrolytes, including new systems and trends in VRFB electrolyte development, have been reported in several reviews [5–7], but the role of counter ions has not been considered systematically. Information about the suitability of various acids as a matrix for VRFB electrolyte is contradictory. The electrolytes based on oxalic acid [8], neat hydrochloric acid [9], or mixtures of sulfuric and hydrochloric acids [10] are reported in the literature. At the same time, oxalic acid is unsuitable as an additive for the V(V) electrolyte because of its reducing ability. For example, ammonium oxalate is instead used as a rebalancing agent producing $CO_2$ on reaction with V(V) to form V(IV) [11]. Previously, the V(V)/V(IV) couple was investigated for use in the positive half-cell of a VRFB [12], and was considered unsuitable in combination with hydrochloric acid due to chlorine gas evolution and the formation of V(IV).

Another reason to explore new VRFB chemistries is the need to improve the thermal stability of the V(V) electrolyte, which is prone to precipitation at elevated temperatures [5,11]. There are several methods to increase the thermal stability of VRFB catholyte: application of additives [11], increase of the proton concentration by increasing the total concentration of sulfuric acid [13], or using methane sulfonic acid in higher concentrations [14], and complexation of V(V) species by chloride ions in mixed acid electrolytes [10]. It is difficult to differentiate between the proton and counter ion effects experimentally especially because the concentration of free acid remains unknown or varies with the state-of-charge (SoC) of the electrolyte.

This study is an attempt to investigate the electrochemical characteristics of V(V)/V(IV) and V(III)/V(II) couples for comparison in sulfuric and hydrochloric acids, which are the most commonly used acids for VRFB electrolytes. Since the distribution of counter ions and protons between the catholyte and anolyte during the charging of vanadium electrolyte is unknown, the conductivity of electrolyte samples obtained by electrolysis of V(IV) or 1:1 mol mixture of V(III) and V(IV) solutions (denoted as $V^{3.5+}$) are considered in this study. The concentrations of the acids were chosen to target the same conductivity of the initial V(IV) electrolyte solutions and the total vanadium concentration was set to be about 1.6 M for both acids.

## 2. Results and Discussion

### *2.1. Electrolyte Preparation*

The electrolyte samples were prepared in $H_2SO_4$ and HCl acids using either V(IV) or $V^{3.5+}$ solution containing equimolar mixtures of V(IV) and V(III) as the initial electrolyte (Section 3.2). The abbreviations of the vanadium electrolyte samples used in the study and their analysis data are given in Table 1 and are defined in Section 3.2.

To obtain V(IV) and $V^{3.5+}$ samples in a HCl matrix, stoichiometric amounts of $VCl_3$, $V_2O_5$, and HCl were calculated based on the reaction:

$$2VCl_3 + V_2O_5 + 2HCl \rightarrow 4VOCl_2 + H_2O \quad (3)$$

Despite the stoichiometric ratios of the reagents, the I-V4-HCl sample contained 4.4% of V(V) possibly because when $VCl_3$ is used as a source of V(III), it is prone to oxidation and its dissolution in HCl (even without $V_2O_5$) resulted in the presence of 3 to 10% mol of a V(IV) fraction. To prepare the II-V3.5-HCl sample, an excess of $VCl_3$ was taken to first produce a 2.2 M $V^{3.5+}$ stock solution, which was then diluted by 3 M HCl to a solution containing 1.6 M of vanadium species (II-V3.5-HCl) (Section 3.2). Such variation in the preparation procedure led to a difference between the total chloride concentration and finally the conductivity of the samples in series I and II (Table 1). The final total chloride concentrations in the electrolytes I-V4-HCl and II-V3.5-HCl were 6.1 M and 7.6 M based on the gravimetric analysis data, respectively. The conductivity of I-V4-HCl solution was 330 $mS \cdot cm^{-1}$. This value is almost two times lower than the conductivity of vanadium-free 3 M HCl solution (Table 1). This

difference can be caused by ion-pairing and incomplete dissociation of vanadium species in electrolyte solution, similar to the interactions assumed to occur in sulfuric acid VRFB electrolyte [15], or because the factual concentration of the free HCl in the vanadium electrolyte samples was lower than 3 M.

To obtain the V(IV) solution with the same conductivity from vanadyl sulfate, 3 M $H_2SO_4$ was used as a matrix (sample I-V4-$H_2SO_4$). Vanadium-free 3 M $H_2SO_4$ solution showed higher conductivity than 3 M HCl. However, these values still correlate with the fact that dissociation of 3 M $H_2SO_4$ proceeds mostly during the first step in solutions with high sulfate concentrations, i.e., containing 1.6 M vanadium species [15,16]. Total sulfate concentration in I-V4-$H_2SO_4$ solution was 4.7 M and corresponded to the common total sulfate concentration of some commercial electrolytes.

**Table 1.** Denotations and analysis data for vanadium electrolyte samples used in the study.

| Sample | Total V Conc. (M) | Molar Content (%) | | | Total Counter Ion Conc. (M) | Conductivity (mS·cm$^{-1}$) | Comment |
|---|---|---|---|---|---|---|---|
| | | V(III) | V(IV) | V(V) | | | |
| I-V4-$H_2SO_4$ ** | 1.66 | | 100 | | 4.7 | 330 | 3 M free $H_2SO_4$ |
| I-V3-$H_2SO_4$ | 1.63 | 100 | | | | 230 | |
| I-V5-$H_2SO_4$ | 1.61 | | 1.5 | 98.5 | | 450 | |
| I-V3.5-$H_2SO_4$ | 1.65 | 45.9 | 54.1 | | | 270 | |
| I-V4-HCl ** | 1.63 | | 95.6 | 4.4 | 6.1 | 330 | targeted 3 M |
| I-V3-HCl | 1.67 | 98.8 | 1.2 | | | 160 | free HCl |
| I-V5-HCl | 1.59 | | 1.7 | 98.3 | | 480 | freshly prepared |
| I-V3.5-HCl | 1.66 | 47.2 | 52.8 | | | 240 | |
| II-V4-HCl | 1.57 | | 100 | | | 365 | |
| II-V3-HCl | 1.68 | 93.1 | 6.9 | | | 240 | |
| II-V5-HCl | 1.54 | | 1.7 | 98.3 | | 490 | freshly prepared |
| II-V3.5-HCl ** | 1.60 | 47.5 | 52.4 | | 7.6 | 320 | |
| 3 M $H_2SO_4$ | | | | | 3 | 810 | |
| 3 M HCl | | | | | 3 | 710 | |

** Prepared by dissolution of vanadium salts and used as a source for other oxidation forms (Section 3.2).

Though the exact vanadium speciation in electrolyte solution is unknown and can involve dimeric V(V) species [4], the process of V(IV) electrolysis can be commonly represented by the following conversions:

$$\text{(cathode) } VO^{2+} + H_2O - e^- \rightarrow VO_2{}^+ + 2H^+ \quad (4)$$

$$\text{(anode) } VO^{2+} + 2H^+ + e^- \rightarrow V^{3+} + H_2O \quad (5)$$

where the protons are consumed in the anolyte and are formed at the catholyte. According to this, the conductivity of I-V3-$H_2SO_4$ is lower and that of I-V5-$H_2SO_4$ is higher compared with the initial I-V4-$H_2SO_4$ solution. In the case of HCl samples (series I), the depletion of protons in the anolyte, i.e., in I-V3-HCl, is more pronounced than in $H_2SO_4$. The conductivity of I-V5-HCl is 30 mS·cm$^{-1}$ higher than that of I-V5-$H_2SO_4$ solution.

Finally, the I-V3.5 sample obtained by mixing the I-V3 and I-V4 forms was characterised by the conductivity of 270 and 240 mS·cm$^{-1}$ for $H_2SO_4$ and HCl, respectively. In contrast, the chemically prepared II-V3.5-HCl solution exhibited higher conductivity (320 mS·cm$^{-1}$); therefore, II-V4-HCl and II-V3-HCl were more conductive than I-V4-HCl and I-V3-HCl. This shows that the factual free HCl concentration in the series II is higher compared to series I, since the total vanadium concentration is the same. Both series I and II of electrolyte samples in HCl were compared with series I in $H_2SO_4$ regarding the electrochemical features.

### 2.2. UV-Vis Spectroscopy

We completed an optical spectroscopy study to evaluate whether the species of V(IV) or V(III) complexed with counter ion were present in electrolyte samples.

V(III) normally exists as an octahedral hexa-aqua cation $[V(H_2O)_6]^{3+}$ in diluted acidic aqueous solutions [17]. The electronic absorption spectrum of V(III) species in non-complexing media such as perchloric acid solutions shows two absorption bands with maximum absorption at 400 and 590 nm [18]. The peaks can be attributed to the $^3T_{1g}(F) \rightarrow {}^3T_{1g}(P)$ transition at around 400 nm and the $^3T_{1g}(F) \rightarrow {}^3T_{2g}$ transitions at around 600 nm. At high acid concentrations, the water molecules from the vanadium solvation sphere can be substituted by chloride or sulfate anion in acidic media [18,19]. Both the V(III) spectra in $H_2SO_4$ (I-V3-$H_2SO_4$) or in HCl (I-V3-HCl and II-V3-HCl) (Figure 1a) exhibited a bathochromic shift, indicating the presence of complexed vanadium species in all the samples. Another indication of a coordination of chloride and sulfate was found in the peak shape of the $^3T_{1g}(F) \rightarrow {}^3T_{1g}(P)$ transition (Figure 1a). The peak features a non-Gaussian shape. One possible explanation of this irregular peak shape could be a slight trigonal distortion of the inner coordination sphere of the V(III) ion. The wavelengths of maximum absorption for V(III) and V(IV) electrolyte samples are summarized in Table 2. Similar values of absorption maxima were reported previously by Vijayakumar et al. [3] for 1.5 M V(III) solutions in pure chloride and sulfate acidic media. The spectra for I-V3-HCl and II-V3-HCl solutions show the same features, even though the difference in conductivities between these electrolytes is about 80 $mS \cdot cm^{-1}$ and II-V3-HCl contained 7% of V(IV) (Table 1). This may indicate the difference in the amount of free HCl rather than the difference in the V(III) speciation.

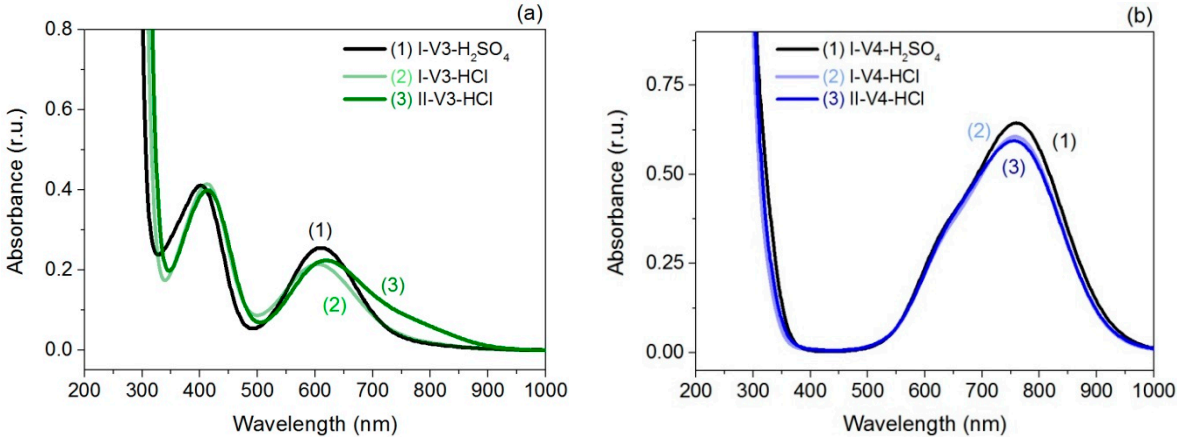


**Figure 1.** Electronic absorption spectra for (**a**) anolyte and (**b**) catholyte samples.

The dissolution of $VOSO_4$ in an acidic aqueous solution yields the hydrated vanadyl cation $[VO(H_2O)_5]^{2+}$, commonly abbreviated as $VO^{2+}$ [17]. For the V(IV) electrolytes, the transitions of the vanadyl ion are usually attributed according to the model of Ballhausen and Gray [20]. The broad peak around 760 nm (Figure 1b) can be attributed to the $^2B_2 \rightarrow {}^2E(I)$ transition as the most intense transition. The shoulder at 630 nm can be assigned to the vibronically allowed $^2B_2 \rightarrow {}^2B_1$ transition. The exact values for each electrolyte are summarized in Table 2. Since I-V4-HCl solution contained 4.4% of V(V) (Table 1), an equivalent amount of I-V3-HCl solution was added to the I-V4-HCl to remove the traces of V(V) before the spectrum was recorded. The HCl electrolytes (series I and II) as well as the $H_2SO_4$ exhibited the same wavelength for both transitions. This is in accordance with the assumptions that the coordination sphere of V(IV) remained unchanged in both of the electrolyte media and counter ions were only weekly bound to the $VO^{2+}$ core [21].

**Table 2.** Spectrophotometric data for vanadium(III) and vanadium(IV) species in various electrolyte matrixes.

| Sample | V(III) | | V(IV) | |
|---|---|---|---|---|
| | $^3T_{1g}(F) \rightarrow {}^3T_{1g}(P)$ | $^3T_{1g}(F) \rightarrow {}^3T_{2g}$ | $^2B_2 \rightarrow {}^2B_1$ | $^2B_2 \rightarrow {}^2E(I)$ |
| I-V3-$H_2SO_4$, I-V4-$H_2SO_4$ | 403 nm | 610 nm | 633 nm | 760 nm |
| I-V3-HCl, I-V4-HCl | 413 nm | 605 nm | 633 nm | 760 nm |
| II-V3-HCl, II-V4-HCl | 414 nm | 620 nm | 633 nm | 760 nm |

To conclude, the chemical state of the V(III) species, i.e., the anolyte of VRFB, is more sensitive to the nature of the counter ion or acid in the electrolyte composition than the V(IV) form or catholyte of VRFB. The presence of chloride or sulfate anions in the inner coordination sphere of V(III) in I-V3-HCl, II-V3-HCl, and I-V3-$H_2SO_4$ samples was confirmed by electronic optical spectroscopy.

### 2.3. Cyclic Voltammetry

The cyclic voltammograms for V(III) and V(IV) electrolyte samples are usually characterized by quasi-reversible V(V)/V(IV) and V(III)/V(II) redox transitions [22,23]. Typical cyclic voltammograms for V(III) and V(IV) electrolyte samples at an oxidatively pre-treated glassy carbon electrode are presented in Figure 2. This pre-treatment was necessary because the voltammetric response in the solution containing V(III) and V(IV) species in sulfuric acid is sensitive to the pre-conditioning of the electrode [24,25].

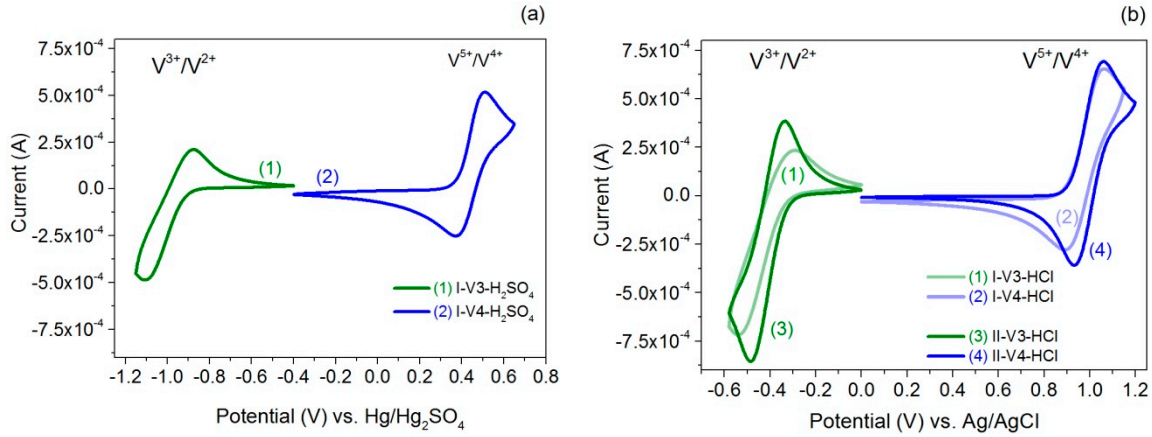


**Figure 2.** Cyclic voltammograms recorded at 20 $mV \cdot s^{-1}$ at a pre-treated glassy carbon electrode in the electrolyte samples of V(III) and V(IV) in (**a**) $H_2SO_4$ and (**b**) HCl media.

All the voltammograms were considered further in terms of peak separation ($\Delta E$) and half-wave potentials ($E_{1/2}$) (Table 3). The $E_{1/2}$ values are calculated as a mid-point potential of anodic and cathodic peaks (($E_{pa} + E_{pc}$)/2) and can be taken as the formal potential ($E^{0'}{}_f$), if the diffusion coefficients of the species in reduced and oxidized states are similar ($D_{red} = D_{ox}$) [25]. Whether this requirement can be fulfilled depends on the exact vanadium speciation, which remains unknown. However, if following common practice, the $E_{1/2}$ values are taken as the formal potentials for the vanadium redox couples, then the theoretical cell voltage under open-circuit conditions is determined by the difference in $E_{1/2}$ for cathodic and anodic couples. As such, we obtained the open-circuit cell voltage ($U_{cell,theor}$) value of 1.43 V for the electrolyte in $H_2SO_4$ (I-V3.5-$H_2SO_4$). The values of $U_{cell,theor}$ for other electrolyte samples are shown in Table 3. In the case of HCl electrolyte series I, the cell voltage was calculated to be lower (1.39 V). The redox potential of the V(V)/V(IV) couple in II-V4-HCl electrolyte solution is 20 mV higher than the value for I-V4-HCl sample. This may be correlated with the fact that the II-V4-HCl has a small excess of free acid compared to I-V4-HCl, as mentioned in Section 2.1. Since the redox potential of

the V(V)/V(IV) couple is proton-dependent, the increase in HCl concentration would cause the $E^{0'}{}_f$ to shift to higher values. The difference between the $E_{1/2}$ values for the V(III)/V(II) couple in I-V3-HCl and II-V3-HCl electrolytes is insignificant considering the usual error of the redox potential estimation by cyclic voltammetry (about 10 mV). Though the $E^{0'}{}_f$ of V(III)/V(II) redox transition is commonly expected to be influenced by the complexation of V(III) species with chloride ions, the theoretical cell voltage under open-circuit conditions for series II in HCl matrix is 1.41 V and very close to that in $H_2SO_4$.

**Table 3.** Electrochemical characteristics of redox couples of anolyte and catholyte: half-wave potential ($E_{1/2}$) and peak-to peak separation (ΔE).

| Sample | Redox Couple | $E_{1/2}$ (V) vs. Ag/AgCl | $E_{1/2}$ (V) vs. $Hg/Hg_2SO_4$ | ΔE (V) | $U_{cell,\ theor.}$ (V) |
|---|---|---|---|---|---|
| I-V3-$H_2SO_4$ | V(III)/V(II) | | −0.99 | 0.23 | 1.43 |
| I-V4-$H_2SO_4$ | V(V)/V(IV) | | 0.44 | 0.13 | |
| I-V3-HCl | V(III)/V(II) | −0.42 | | 0.25 | 1.39 |
| I-V4-HCl | V(V)/V(IV) | 0.97 | | 0.16 | |
| II-V3-HCl | V(III)/V(II) | −0.41 | | 0.14 | 1.41 |
| II-V4-HCl | V(V)/V(IV) | 1.00 | | 0.13 | |

The V(V)/V(IV) couple was characterized by the peak-to-peak separation (ΔE) value of 0.13–0.16 V in all the electrolytes: I-V4-HCl, II-V4-HCl, and I-V4-$H_2SO_4$ (Table 3). These solutions are comparable regarding the conductivity (Table 1). Generally, the ΔE is affected by both the uncompensated ohmic drop between working and reference electrodes (which is proportional to the electrolyte conductivity) and by the kinetics of the redox reaction. Since the conductivity of I-V3-$H_2SO_4$ solution was higher than that of I-V3-HCl (Table 1), it is difficult to differentiate between these two factors. However, the V(III)/V(II)redox couple in solutions with the same conductivity, I-V3-$H_2SO_4$ and II-V3-HCl, was characterized by a lower ΔE value in the HCl matrix in contrast with $H_2SO_4$. This can be attributed to the difference in the coordination sphere due to complexation (Section 2.2).

Even if the total concentration of vanadium species in HCl and $H_2SO_4$ samples is similar (Table 1), peak currents of voltammograms in HCl series I and II are higher than those in $H_2SO_4$ (Figure 2). Since the $H_2SO_4$ and HCl have different viscosities, the difference in peak currents is hardly possible to be attributed to the difference in diffusion coefficients of vanadium species. The lower peak currents may also be associated with the presence of more than one complex species in solution that have slightly different redox potentials, also leading to the broadening of the peaks.

To investigate the characteristics of the electrolyte under current flow conditions, i.e., battery operation conditions, charge-discharge tests were to be performed using HCl and $H_2SO_4$ electrolytes.

### *2.4. Cell Test*

The typical charge-discharge cycles for the cells operated with HCl and $H_2SO_4$ vanadium electrolytes in $V^{3,5+}$ oxidation form are presented in Figure 3. The ohmic resistance of these cells was verified by electrochemical impedance measurements before charging, which was about 70 mOhm for all cells despite the difference in electrolyte conductivities of 30–80 $mS{\cdot}cm^{-1}$ (Table 1). Both charge and discharge voltages ($U_{cell}$) were in the range of 1.50 to 1.55 V and 1.21 to 1.23 V, respectively, and the voltage efficiency was 78% for I-V3.5-$H_2SO_4$ and 80% for I-V3.5-HCl and II-V3.5-HCl electrolytes (Figure 3). The small difference in the theoretical cell voltage, which was expected based on the cyclic voltammetry data, is correlated with the values of cell voltage $U_{cell}$ obtained during cell operation. The cells exhibited coulombic and energy efficiencies of 90–97% and 72–77%, respectively (Table 4). The values of coulombic efficiency were common for VRFB and consistent with the characteristics reported in the literature [9]. However, the values of coulombic and energy efficiency for the I-3.5-HCl were the lowest compared to II-V3.5-HCl and I-V3.5-$H_2SO_4$.

To further reveal the differences between the cells with HCl- and $H_2SO_4$-based electrolytes, the correlation between $U_{cell}$, half-cell, and redox potentials was considered. The cell voltage can be described as follows [26]:

$$U_{cell} = \varphi_C - \varphi_A + IR_{cell} + \varphi_{memb} \quad (6)$$

where I is the current, $R_{cell}$ is the ohmic resistance of the cell, and $\varphi_{memb}$ is the membrane potential.

The sum of $IR_{cell}$ and $\varphi_{memb}$ is therefore determined by the term $U_{cell} - (\varphi_C - \varphi_A)$, as derived from Equation (6). If $IR_{cell}$ is equal due to the same cell materials and chosen concentration of acids to target similar electrolyte conductivity, the difference in $U_{cell} - (\varphi_C - \varphi_A)$ should be related to the membrane potential $\varphi_{memb}$. Table 4 shows that the $U_{cell} - (\varphi_C - \varphi_A)$ values are similar for both of the HCl and $H_2SO_4$ systems during the charge and discharge step within the error of the experiment. The variance in the values given in Table 4 were due to variations in the cycles and correspond to a standard deviation from the average value.

Half-cell potentials can be expressed as follows:

$$\varphi_C = \varphi_{C,redox} + \eta_{act(C)} + \eta_{con(C)} \quad (7a)$$

$$\varphi_A = \varphi_{A,redox} + \eta_{act(A)} + \eta_{con(A)} \quad (7b)$$

where $\eta_{con(C)}$ and $\eta_{con(A)}$ are the concentration overpotentials for the cathode and anode, respectively; and $\eta_{act(C)}$ and $\eta_{act(A)}$ are the activation overpotentials for cathodic and anodic reactions, respectively. The sum of the overpotentials $\eta_{act} + \eta_{con}$ for the cathode and anode can then be estimated from the terms $(\varphi_C - \varphi_{C,redox})$ and $(\varphi_A - \varphi_{A,redox})$ in Equations (7a) and (7b), respectively, which were calculated as average values from the charge-discharge cycle, which are shown in Table 4. $(\varphi_C - \varphi_{C,redox})$ is about 20 to 30 mV for the charge and discharge processes for all the cells, i.e., with HCl and $H_2SO_4$ electrolytes.

As for the anodic reaction, the term $(\varphi_A - \varphi_{A,redox})$ reaches values of 30–60 mV for charge and discharge steps in the case of I-V3.5-$H_2SO_4$ and I-V3.5-HCl electrolytes, i.e., higher than II-V3.5-HCl. Since $\eta_{con(C)}$ and $\eta_{con(A)}$ mostly depend on the cell construction and operation mode, which were the same for the HCl and $H_2SO_4$ systems, the major contribution to the difference between the $(\varphi_A - \varphi_{A,redox})$ term was expected from the anodic activation overpotential $(\eta_{act(A)})$. This may indicate the slower kinetics of the anodic reaction (V(III)/V(II) conversion) in the case of I-$H_2SO_4$ and I-HCl systems compared with II-HCl. Higher peak-to-peak separation for the V(III)/V(II) couple in I-V3-$H_2SO_4$ and I-V3-HCl than in II-V3-HCl (Table 3) is correlated with the $(\varphi_A - \varphi_{A,redox})$ values.

Except for the differences in the activation for the anodic reaction, the charge-discharge characteristics of the cells with HCl and $H_2SO_4$ electrolytes used in this work reveal no considerable difference.

**Table 4.** Parameters for the cells evaluated in the cell test for HCl (I-V3.5-HCl, II-V3.5-HCl) and $H_2SO_4$ (I-V3.5-$H_2SO_4$) vanadium electrolytes.

| Parameter | I-V3.5-$H_2SO_4$ | | I-V3.5-HCl | | II-V3.5-HCl | |
|---|---|---|---|---|---|---|
| | Charge | Discharge | Charge | Discharge | Charge | Discharge |
| $\varphi_A - \varphi_{A,\,redox}$ (V) ** | −0.04 ± 0.01 | 0.06 ± 0.02 | −0.05 ± 0.01 | 0.03 ± 0.01 | −0.02 ± 0.01 | 0.02 ± 0.01 |
| $\varphi_C - \varphi_{C,\,redox}$ (V) ** | 0.03 ± 0.01 | −0.02 ± 0.01 | 0.02 ± 0.01 | −0.02 ± 0.01 | 0.03 ± 0.01 | −0.03 ± 0.01 |
| $U_{cell} - (\varphi_C - \varphi_A)$ (V) ** | 0.09 ± 0.01 | −0.10 ± 0.01 | 0.080 ± 0.01 | −0.10 ± 0.01 | 0.10 ± 0.01 | −0.11 ± 0.01 |
| Capacity (Ah·$L^{-1}$) * | 15.7 | 15.3 | 17.5 | 15.7 | 14.8 | 13.9 |
| Energy (Wh·$L^{-1}$) * | 24.1 | 18.5 | 26.5 | 19.0 | 22.7 | 17.1 |
| Coulombic efficiency (%) | 97 | | 90 | | 94 | |
| Energy efficiency (%) | 77 | | 72 | | 75 | |

* For the second cycle, ** the average value for three consecutive cycles.

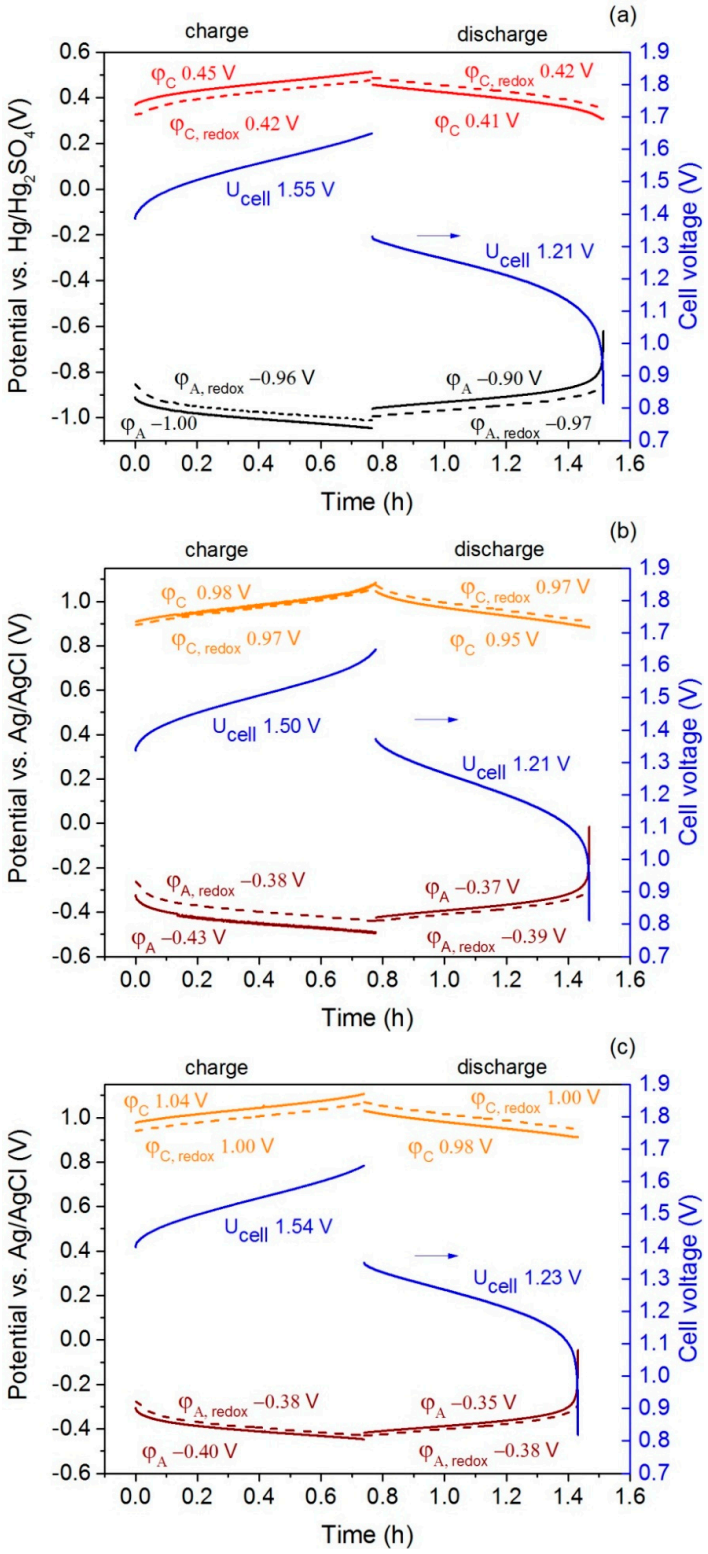


**Figure 3.** Charge-discharge curves for cells operated with (**a**) I-V3.5-$H_2SO_4$, (**b**) I-V3.5-HCl, and (**c**) II-V3.5-HCl electrolytes at a current density of 50 mA·cm$^{-2}$. Cell voltage curves (blue lines), cathodic $\varphi_C$ and anodic $\varphi_A$ half-cell potentials (solid lines), cathodic $\varphi_{C,\,redox}$ and anodic $\varphi_{C,\,redox}$ redox potentials (dashed lines).

Further cyclic performance of the cells was tested under conditions that are more closely related to common protocol. The cells were charged and discharged at the current density of 50 $mA \cdot cm^{-1}$, though we did not maintain the cell at open-circuit potential between the charge-discharge cycles. The end-of-charge and discharge voltages were set to 1.65 V and 0.8 V, respectively, for all cells, though the expected open-circuit cell voltage (from the formal potentials, Table 3) for I-V3.5-$H_2SO_4$ system should have been 20–40 mV higher than for the cell with I-V3.5-HCl and II-V3.5-HCl electrolytes. The capacity of the cell with II-V3.5-$H_2SO_4$ degraded to 50% of its initial value after 19 cycles under these conditions (Figure 4) and crossover of electrolyte occurred, leading to a variation in the electrolyte volumes in the anodic and cathodic tanks.

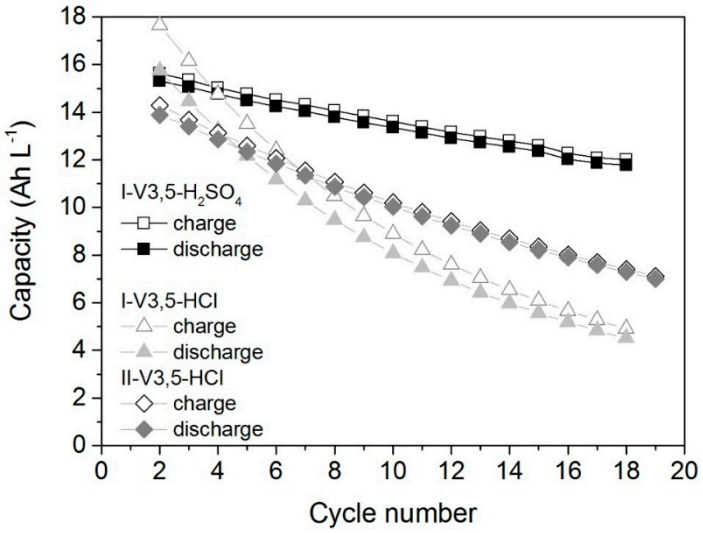


**Figure 4.** Cyclability of the cell operated with I-V3.5-$H_2SO_4$, I-V3.5-HCl, and II-V3.5-HCl electrolytes.

Higher capacity loss during continuous charge-discharge cycling i.e., to 30% of the initial value, was also detected in the case of the I-V3.5-HCl electrolyte. The crossover of the electrolyte was more pronounced and traces of an orange solid substance, probably vanadium pentoxide, were observed at the membrane after the cell was disassembled. Compared to the II-V3.5-HCl electrolyte, the I-V3.5-HCl electrolyte retained only 30% of the initial capacity and a large amount of the orange deposit was observed on the membrane at the end of the test. As the main difference between the I-V3.5-HCl and II-V3.5-HCl systems is in their conductivity (at constant total vanadium concentration), the stronger capacity decay in the case of I-V3.5-HCl can be assigned to the lower protons or free acid concentration in this electrolyte samples compared to II-V3.5-HCl or I-V3.5-$H_2SO_4$.

### *2.5. Thermal Stability*

The poor thermal stability of the catholyte at state-of-charges (SoC) higher than 80% is a well-known issue for electrolytes based on sulfuric, methane sulfonic acids, or mixtures of both [5]. As for the vanadium electrolyte containing HCl, there are two concerns about chlorine evolution: (1) electrochemical chlorine evolution from the supporting electrolyte, especially if the cell is overcharged, and (2) chemical generation of chlorine from HCl due to its oxidation by V(V). The electrochemical chlorine evolution depends on the cell operation protocol and should not appear unless a large overpotential is applied. To avoid misinterpretation and to assess the thermal stability of V(V) electrolytes at elevated temperatures, it was first necessary to check its chemical stability at room temperature. Otherwise, a possible chemical reduction of V(V) in the case of reducible supporting electrolyte anions would lead to a decrease in the SoC of the catholyte and to an increase in induction time for the thermally-induced precipitation of the V(V) species. For this purpose, we analysed the V(V) samples of electrolytes (I-V5-$H_2SO_4$, I-V5-HCl, and II-V5-HCl), which were prepared by electrolysis (Table 1), by titration after storage at room temperature for several weeks and after the sample was

kept at 45 °C. The titration data of the I-V5-$H_2SO_4$ sample remained unchanged at 98% of SoC at room temperature for least six weeks (Table 5). After exposure of I-V5-$H_2SO_4$ to 45 °C for one day, only traces of precipitate formation could be observed; however, the total vanadium concentration and SoC remained unchanged. The decrease in the total vanadium concentration to 1.4 M and precipitation was observed in the sample after a two days exposure to 45 °C.

**Table 5.** Titration results for the catholyte samples with a HCl and $H_2SO_4$ matrix.

| Sample | Conditions | Total V Concentration (M) | Molar Content (%) | | Comment |
|---|---|---|---|---|---|
| | | | V(IV) | V(V) | |
| I-V5-$H_2SO_4$ | initial | 1.61 | 1.5 | 98.5 | |
| | after 3 weeks at RT | 1.62 | 1.4 | 98.6 | unchanged |
| | after 6 weeks at RT | 1.62 | 1.6 | 98.4 | unchanged |
| | after 1 day at 45 °C | 1.62 | 2 | 98.0 | traces of precipitate |
| | after 5 weeks at RT and 2 days at 45 °C | 1.40 | 1.8 | 98.2 | precipitation |
| I-V5-HCl | initial | 1.59 | 1.7 | 98.3 | |
| | after 3 weeks at RT | 1.60 | 3.1 | 97.0 | SoC shift |
| | after 6 weeks at RT | 1.59 | 4.0 | 96.0 | SoC shift |
| | after 1 day at 45 °C | 1.55 | 4.1 | 95.9 | precipitation |
| | after 5 weeks at RT and 2 days at 45 °C | 1.40 | 6.0 | 94.0 | precipitation |
| II-V5-HCl | initial | 1.54 | 1.7 | 98.3 | |
| | after 3 weeks at RT | 1.52 | 5.4 | 94.6 | SoC shift |
| | after 5 weeks at RT | 1.53 | 7.3 | 92.7 | SoC shift |
| | after 1 day at 45 °C | 1.54 | 9.0 | 91.0 | SoC shift |
| | after 4 weeks at RT and 2 days at 45 °C | 1.53 | 11.4 | 88.6 | SoC shift |

The reference sample of I-V5-HCl, which was stored at room temperature, showed a slight shift in SoC (by 1% during the three weeks and 2% after six weeks). The precipitation of vanadium pentoxide at 45 °C, with a measurable decrease in the total vanadium concentration, and shift in the SoC from 98 to 96% occurred in the sample I-V5-HCl after one day. Further decrease in SoC and more considerable formation of vanadium pentoxide occurred when the sample was kept over two days at 45 °C after storage at room temperature for five weeks. In comparison, the process of the V(V) reduction is faster in II-V5-HCl. However, there was no change in the total vanadium concentration and no deposition of vanadium pentoxide.

The SoC for II-V5-HCl at room temperature decreased to 94.6% (by 4%) over three weeks. The SoC decreased to 91% when the freshly prepared sample II-V5-HCl was heated to 45 °C. The II-V5-HCl sample, which was stored five weeks at room temperature, exhibited a further SoC shift by almost 10% after exposure to 45 °C for a week. If the decrease in the SoC can be attributed to the reduction of V(V) species by chloride ions, it should be dependent, among others, on the formal potential of the V(V)/V(IV) couple and on the amount of free acid, i.e., the activity of protons. The I-V5-HCl and II-V5-HCl samples, which were characterized by different conductivities (and presumable proton concentrations), exhibited different stabilities after exposure to elevated temperature. The fact that the reduction of V(V) to V(IV) proceeded faster is correlated with the redox potentials of the V(V)/V(IV) couple in HCl electrolyte of series I and II (Table 3). The absence of precipitate in II-V5-HCl electrolyte is likely due either to the decrease in SoC or to higher free acid concentration , rather than to the nature of the counter ion.

Generally, to address the question of V(V) chemical stability in HCl at given concentrations, it is necessary to consider the difference in the redox potentials of the V(V) reduction and chloride oxidation under real battery relevant conditions. The precise values of activity coefficients or information about the chemical state of reacting species in an electrolyte solution should be known to find the thermodynamic conditions required for electrolyte stability. Otherwise, the limit of the SoC of less than 100% in the case of HCl-based electrolytes (at least at 1.6 M vanadium and 6–7.6 M total chloride concentrations) appears to be the easiest condition to avoid chlorine evolution due to the reaction of V(V) with chloride ions. A VRFB operated with $H_2SO_4$-containing electrolyte is also known to have a limit of less than 80% SoC due to the thermal aging of the catholyte at elevated temperatures [4].

For electrolytes with 1.6 M total vanadium concentration, the application of HCl as an electrolyte matrix requires the careful control of the free acid concentration. The increase in the concentration of free acid can result in the shift of the formal potential of the V(V)/V(IV) redox couple to higher values and favor the chemical oxidation of chloride ions. Low concentrations of free acid lead to the precipitation of vanadium pentoxide at elevated temperatures, similar to the behavior of vanadium electrolyte in sulfuric acid. Regarding the electrochemical parameters of the cell operation, both electrolyte matrixes, HCl and $H_2SO_4$, were comparable, provided that the total vanadium concentration and conductivity of the electrolyte samples were equal.

## 3. Materials and Methods

### *3.1. Chemicals*

Sulfuric acid (95%, supra) and hydrochloric acid (32%, p.a.) were Carl-Roth (Karlsruhe, Germany) reagents. Vanadium pentoxide (98%) and vanadyl sulfate hydrate (technical grade), purchased from Chempur (Karlsruhe, Germany), were used without purification. The amount of crystallization water in $VOSO_4 \cdot xH_2O$ was determined by potentiometric titration. Vanadium(III) chloride (97%) was used as a Sigma-Aldrich and Merck (EMD Millipore, Burlington, MA, USA) reagent. The commercial standard solution for conductivity measurements was obtained from Carl-Roth (Karlsruhe, Germany).

### *3.2. Electrolyte Preparation*

The two pathways used to produce the electrolyte samples in various oxidation states are shown in Figure 5. V(III) and V(V) oxidation states of electrolyte in $H_2SO_4$ were prepared by the electrolysis of vanadyl sulfate dissolved in $H_2SO_4$ (sample I-V4-$H_2SO_4$). In the case of HCl, both Scheme I and II were used. For both series of samples in HCl matrix, the preparation procedure was based on the comproportionation of V(III) and V(V). For this reaction, $VCl_3$ was first dissolved in 3 M HCl solution with subsequent addition of stoichiometric amounts of $V_2O_5$ and concentrated HCl (Table 6). $V_2O_5$ was used in an amount so that the resulting solution contained either V(IV) (series I, I-V4-HCl) or mixture of V(III) and V(IV) in a 1:1 molar ratio (series II, II-V3.5-HCl). The total concentration of chloride in the samples I-V4-HCl and II-V3.5-HCl was determined gravimetrically.

The V(IV) solutions in series I (I-V4-HCl, I-V4-$H_2SO_4$) were subjected to electrolysis to prepare the V(III) (I-V3-HCl, I-V3-$H_2SO_4$) and V(V) (I-V5-HCl, I-V5-$H_2SO_4$) forms. The electrolyte in $V^{3.5+}$ form in series I (I-V3.5-HCl, I-V3.5-$H_2SO_4$), used for the charge-discharge trial, was obtained by mixing the V(III) and V(IV) electrolyte samples in a 1:1 $v/v$ ratio in HCl or $H_2SO_4$ matrix, respectively (Figure 5).

The electrolyte in $V^{3.5+}$ form in series II (II-V3.5-HCl) was first converted into V(III) (II-V3-HCl) and V(IV) (II-V4-HCl) forms, then to V(II) (II-V2-HCl) and V(V) forms (II-V5-HCl) by charging the cell (Figure 5). After this charging step, the charge-discharge cell test was performed for the electrolyte series II cell.

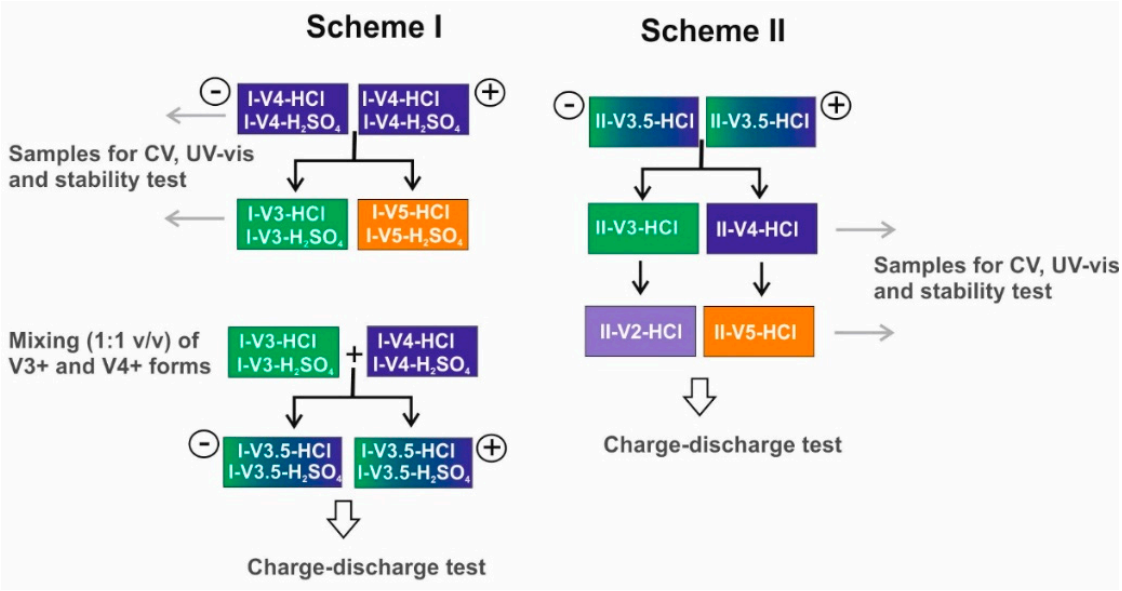


**Figure 5.** Schematic representation of the preparation pathways for electrolyte samples (series I and II).

**Table 6.** The amounts of reagents used for the preparation of initial vanadium electrolyte solutions.

| Sample | $VCl_3$ | $V_2O_5$ | HCl | | Targeted Concentration |
|---|---|---|---|---|---|
| | | | HCl 3 M | HCl 32% w/w | Vanadium |
| I-V4-HCl | 0.4 moles | 0.2 moles | 0.5 L (1.5 moles) | 37 mL (0.4 moles) | 1.6 M |
| II-V3.5-HCl stock * | 0.85 moles | 0.13 moles | 0.5 L (1.5 moles) | 25 mL (0.26 moles) | 2.2 M |
| **Sample** | **$VOSO_4 \cdot 5.1H_2O$** | | **$H_2SO_4$ 95% w/w** | **$H_2O$** | **Targeted concentration** |
| | | | | | **Vanadium** |
| I-V4-$H_2SO_4$ | 204 g (0.8 moles) | | 84 ml (1.5 moles) | to 0.5 L | 1.6 M |

* II-V3.5-HCl was prepared by dilution of the II-V3.5-HCl stock with 3 M HCl.

A 40 $cm^2$ cell with the same design as described for the cell test (Section 3.4) was used for electrolysis. The electrolysis was carried out in galvanostatic-potentiostatic mode with a maximal voltage of 1.65 V and a maximal current of 3 A.

For the cyclic voltammetry investigations in the anodic and cathodic regions of potential, V(III) and V(IV) samples of the electrolyte were used.

### *3.3. Electrolyte Characterization*

#### 3.3.1. Titration and Gravimetric Analysis

The total vanadium concentration and the molar content of vanadium in various redox states in electrolyte samples were determined by potentiometric cerimetric titration. The titration was carried out with 0.1 M cerium(IV) sulfate standard solution using a Titrator T70 (Mettler Toledo Int. Inc., Giessen, Germany).

The concentration of chloride ions in chemically prepared HCl-containing electrolyte samples was determined by gravimetric analysis with silver nitrate.

#### 3.3.2. Conductivity Measurement

We measured the electrolyte conductivity in a four-electrode glass cell with a cell constant of 7.3 $mS \cdot cm^{-1}$ and glassy carbon electrodes. The cell was calibrated with a standard conductivity solution (500 $mS \cdot cm^{-1}$). The AC impedance technique was used in the frequency range from 10 to 100 kHz with AC of 10 mA and 0 DC.

#### 3.3.3. Optical Absorption Spectra (UV-Vis)

The absorbance of vanadium electrolyte samples was recorded with a Shimadzu (Duisburg, Germany) 1650PC ultraviolet-visible (UV-vis) double beam spectrophotometer. These measurements were recorded in matched quartz cuvettes with 0.2 mm optical path length, so that dilution of the samples was not necessary.

#### 3.3.4. Cyclic Voltammetry (CV)

Cyclic voltammetric measurements were recorded in a three-electrode glass cell at room temperature using a Gamry Reference (Warminster, PA, USA) 3000 potentiostat. A platinum plate served as a counter electrode. The voltammograms were recorded and are shown using different scales of potential against reference electrodes containing chloride and sulfate ions to avoid the problem of liquid-junction potential. All potentials in the HCl matrix solutions were measured and reported versus a Ag/AgCl/3 M NaCl reference electrode. A $Hg/Hg_2SO_4/K_2SO_4$(sat.) reference electrode was used to measure the voltammetric response in sulfate-containing electrolyte samples. A glassy carbon disc working electrode (1 mm diameter, ALS, Tokyo, Japan) was polished using diamond pastes (6, 1, and 0.25 µm) and thoroughly washed with water. The working electrode was additionally electrochemically pre-treated after conventional polishing. The electro-oxidative pretreatment of a glassy carbon electrode was completed in a separate three-electrode cell filled with 2 M $H_2SO_4$ solution by application of six cyclic potential scans in the range from 0 to 2.0 V against a Ag/AgCl reference electrode at 20 $mV \cdot s^{-1}$. The final applied potential was 0 V.

#### 3.3.5. Thermal Stability

For thermal stability trials, a climate chamber conditioned at 45 °C (Weiss WKL 64, Reiskirchen-Lindenstruth, Germany) was used to keep 1-mL electrolyte samples in closed vials for a predefined period of time. The molar content of V(V) and V(IV) and total vanadium concentrations were determined afterward by titration. If necessary, the liquid phase was separated from precipitate formed at 45 °C by filtration.

### *3.4. Cell Test*

A charge-discharge cell test was performed in a 40 $cm^2$ cell, which was assembled using a Fumasep FAP-450 anion exchange membrane (FuMa-Tech GmbH, Bietigheim-Bissingen, Germany) as a separator, GFA6 graphite felt (SGL Group, Meitingen, Germany) and FU 4369 graphite bipolar plates (Schunk Kohlenstofftechnik GmbH, Heuchelheim, Germany) were used as electrode and current collector materials, respectively (for details of the cell design, see Noack et al. [27]). The felts were pre-treated for one hour at 400 °C in an oven before the cell assembly. The electrolyte flow rate was 75–80 mL/min.

The high-frequency resistance of the cells was determined before the charge-discharge test using AC impedance with an amplitude of 10 mA at open circuit voltage at a SoC of 0%.

The charge-discharge cell test was performed using a Gamry Reference (Warminster, PA, USA) 3000 potentiostat in galvanostatic mode at 50 mA $cm^{-2}$. The end-of-charge voltage was set to 1.65 V and the end-of-discharge voltage was 0.8 V. To monitor the cathodic ($\varphi_{C,\,redox}$) and anodic ($\varphi_{A,\,redox}$) redox potentials and cathodic ($\varphi_C$) and anodic ($\varphi_A$) half-cell potentials, the cell was equipped with additional glassy carbon electrodes and reference electrodes (Ag/AgCl or $Hg/Hg_2SO_4$, respectively) incorporated into the catholyte and anolyte circuit (Figure 6). Redox potentials and half-cell potentials were measured using additional electrometer channels of the Gamry (Warminster, PA, USA) potentiostat.

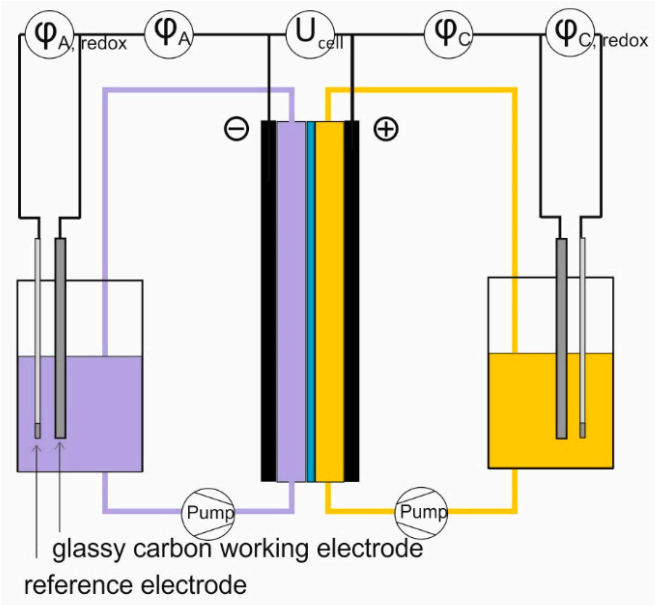


**Figure 6.** Schematic diagram of the electrodes connection for the cell test used to measure the cathodic ($\varphi_{C,\,redox}$) and anodic ($\varphi_{A,\,redox}$) redox potentials, cathodic ($\varphi_C$) and anodic ($\varphi_A$) half-cell potentials, and cell voltage ($U_{cell}$).

## 4. Conclusions

A comparison of 1.6 M vanadium electrolytes, prepared from V(IV) in sulfuric acid (4.7 M total sulfate) and from V(IV) or $V^{3.5+}$ in hydrochloric acid (6.1, 7.6 M total chloride), led us to the following conclusions:

(1) The electrolyte preparation procedures should be considered to differentiate between the proton effect of an acidic matrix and the complexing effect or nature of the counter ions on the electrochemical properties of V(III)/V(II) and V(V)/V(IV) couples, and on the stability of the fully charged V(V) electrolyte at elevated temperatures.

(2) Provided that the electrolyte samples have the same conductivity and total vanadium concentration, the characteristics of the cell operated with these electrolytes (capacity, energy efficiency, and activation losses) are similar. The cyclability of the cell with sulfuric acid electrolyte is better compared to the cells with hydrochloric acid.

(3) V(V) in catholyte at an SoC of 98% in hydrochloric acid undergoes reduction by chloride ions, which can proceed slower or faster depending on the amount of free acid in the electrolyte and the temperature.

**Author Contributions:** Data acquisition and analysis: H.M., M.F., and N.R. Methodology and interpretation: N.R., J.N., P.F. and M.S.-K. Writing—original draft preparation: N.R. and F.P. Writing—review and editing: N.R., J.N., J.T., K.P., and M.S.-K. Supervision: J.T. and K.P.

**Funding:** This research was funded by German Federal Ministry for Economic and Energy (Bundesministerium für Wirtschaft und Energie) grant number (0325755B) and German Federal Ministry of Education and Research (Bundesministerium für Bildung und Forschung) grant number (01DR17027).

**Acknowledgments:** The authors are grateful to Carolyn Fisher for technical assistance in this study.

**Conflicts of Interest:** The authors declare no conflict of interest.

## References


1. Kausar, N.; Howe, R.; Skyllas-Kazacos, M. Raman spectroscopy studies of concentrated vanadium redox battery positive electrolytes. *J. Appl. Electrochem.* **2001**, *31*, 1327–1332. [CrossRef]
2. Rahman, F.; Skyllas-Kazacos, M. Solubility of vanadyl sulfate in concentrated sulfuric acid solutions. *J. Power Sources* **1998**, *72*, 105–110. [CrossRef]
3. Vijayakumar, M.; Li, L.; Nie, Z.; Yang, Z.; Hu, J. Structure and stability of hexa-aqua V(iii) cations in vanadium redox flow battery electrolytes. *Phys. Chem. Chem. Phys.* **2012**, *14*, 10233–10242. [CrossRef] [PubMed]
4. Roznyatovskaya, N.V.; Roznyatovsky, V.A.; Höhne, C.-C.; Fühl, M.; Gerber, T.; Küttinger, M.; Noack, J.; Fischer, P.; Pinkwart, K.; Tübke, J. The role of phosphate additive in stabilization of sulphuric-acid-based vanadium(V) electrolyte for all-vanadium redox-flow batteries. *J. Power Sources* **2017**, *363*, 234–243. [CrossRef]
5. Skyllas-Kazacos, M.; Cao, L.; Kazacos, M.; Kausar, N.; Mousa, A. Vanadium Electrolyte Studies for the Vanadium Redox Battery-A Review. *ChemSusChem* **2016**, *9*, 1521–1543. [CrossRef] [PubMed]
6. Choi, C.; Kim, S.; Kim, R.; Choi, Y.; Kim, S.; Jung, H.-Y.; Yang, J.H.; Kim, H.-T. A review of vanadium electrolytes for vanadium redox flow batteries. *Renew. Sustain. Energy Rev.* **2017**, *69*, 263–274. [CrossRef]
7. Lu, W.; Li, X.; Zhang, H. The next generation vanadium flow batteries with high power density—A perspective. *Phys. Chem. Chem. Phys.* **2018**, *20*, 23–35. [CrossRef]
8. Lee, J.G.; Park, S.J.; Cho, Y.I.; Shul, Y.G. A novel cathodic electrolyte based on $H_2C_2O_4$ for a stable vanadium redox flow battery with high charge-discharge capacities. *RSC Adv.* **2013**, *3*, 21347–21351. [CrossRef]
9. Kim, S.; Vijayakumar, M.; Wang, W.; Zhang, J.; Chen, B.; Nie, Z.; Chen, F.; Hu, J.; Li, L.; Yang, Z. Chloride supporting electrolytes for all-vanadium redox flow batteries. *Phys. Chem. Chem. Phys.* **2011**, *13*, 18186–18193. [CrossRef]
10. Li, L.; Kim, S.; Wang, W.; Vijayakumar, M.; Nie, Z.; Chen, B.; Zhang, J.; Xia, G.; Hu, J.; Graff, G.; et al. A Stable Vanadium Redox-Flow Battery with High Energy Density for Large-Scale Energy Storage. *Adv. Energy Mater.* **2011**, *1*, 394–400. [CrossRef]
11. Cao, L.; Skyllas-Kazacos, M.; Menictas, C.; Noack, J. A review of electrolyte additives and impurities in vanadium redox flow batteries. *J. Energy Chem.* **2018**, *27*, 1269–1291. [CrossRef]
12. Sum, E.; Rychcik, M.; Skyllas-Kazacos, M. Investigation of the V(V)/V(IV) system for use in the positive half-cell of a redox battery. *J. Power Sources* **1985**, *16*, 85–95. [CrossRef]
13. Rahman, F.; Skyllas-Kazacos, M. Vanadium redox battery: Positive half-cell electrolyte studies. *J. Power Sources* **2009**, *189*, 1212–1219. [CrossRef]
14. He, Z.; Li, Z.; Zhou, Z.; Tu, F.; Jiang, Y.; Pan, C.; Liu, S. Improved performance of vanadium redox battery using methylsulfonic acid solution as supporting electrolyte. *J. Renew. Sustain. Energy* **2013**, *5*, 023130. [CrossRef]
15. Skyllas-Kazacos, M.; Kazacos, M. State of charge monitoring methods for vanadium redox flow battery control. *J. Power Sources* **2011**, *196*, 8822–8827. [CrossRef]
16. Fraenkel, D. Electrolytic Nature of Aqueous Sulfuric Acid. 2. Acidity. *J. Phys. Chem. B* **2012**, *116*, 11678–11686. [CrossRef] [PubMed]
17. Crans, D.C.; Tracey, A.S. The Chemistry of Vanadium in Aqueous and Nonaqueous Solution. In *Vanadium Compounds, Chemistry, Biochemistry, and Therapeutic Applications*; Tracey, A.S., Crans, D.C., Eds.; American Chemical Society: Washington, DC, USA, 1998; Volume 711, pp. 2–29.
18. Martin, E.L.; Bentley, K.E. Spectrophotometric Investigation of Vanadium(II), Vanadium(III), and Vanadium(IV) in Various Media. *Anal. Chem.* **1962**, *34*, 354–358. [CrossRef]
19. Pajdowski, L. A spectrophotometric study of the hydrolysis of vanadium (III) ion. *J. Inorg. Nuclear Chem.* **1966**, *28*, 433–442. [CrossRef]
20. Ballhausen, C.J.; Gray, H.B. The Electronic Structure of the Vanadyl Ion. *Inorg. Chem.* **1962**, *1*, 111–122. [CrossRef]
21. Vijayakumar, M.; Burton, S.D.; Huang, C.; Li, L.; Yang, Z.; Graff, G.L.; Liu, J.; Hu, J.; Skyllas-Kazacos, M. Nuclear magnetic resonance studies on vanadium(IV) electrolyte solutions for vanadium redox flow battery. *J. Power Sources* **2010**, *195*, 7709–7717. [CrossRef]
22. Roznyatovskaya, N.; Noack, J.; Fuehl, M.; Pinkwart, K.; Tuebke, J. Towards an all-vanadium redox-flow battery electrolyte: Electrooxidation of V(III) in V(IV)/V(III) redox couple. *Electrochim. Acta* **2016**, *211*, 926–932. [CrossRef]

23. Skyllas-Kazacos, M. Novel vanadium chloride/polyhalide redox flow battery. *J. Power Sources* **2003**, *124*, 299–302. [CrossRef]
24. Noack, J.; Roznyatovskaya, N.; Kunzendorf, J.; Skyllas-Kazacos, M.; Menictas, C.; Tübke, J. The influence of electrochemical treatment on electrode reactions for vanadium redox-flow batteries. *J. Energy Chem.* **2018**, *27*, 1341–1352. [CrossRef]
25. Compton, R.G.; Banks, G.E. *Understanding Voltammetry*, 2nd ed.; Imperial College Press: London, UK, 2011; pp. 2–444, ISBN 9781848165861.
26. Tang, A.; Bao, J.; Skyllas-Kazacos, M. Studies on pressure losses and flow rate optimization in vanadium redox flow battery. *J. Power Sources* **2014**, *248*, 154–162. [CrossRef]
27. Noack, J.; Vorhauser, L.; Pinkwart, K.; Tübke, J. Aging Studies of Vanadium Redox Flow Batteries. *ECS Trans.* **2011**, *33*, 3–9.